M2 INTERNSHIP REPORT

Light propagation in a 1D dispersive media

Student : Noé Grenier
Supervisors : Prof. Quentin Glorieux and PhD Alix Merolle

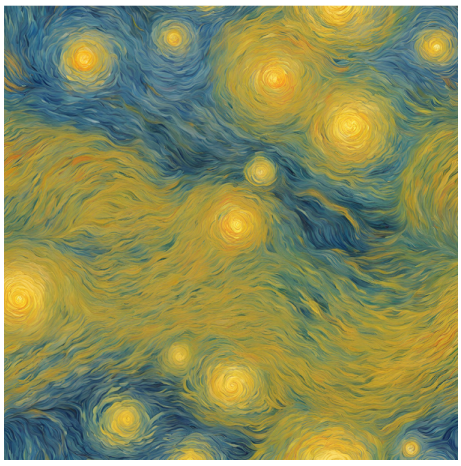

"Light propagation in a dispersive medium in a Van Gogh style"

Quantum Fluids of Light Team
April 2024 - June 2024

Contents

Context

I joined the lab at the beginning of April 2024 for a three-month internship. The lab has a large team dedicated to studying quantum fluids of light using hot Rubidium cells. When I arrived, a relocation of the entire lab was scheduled for early June, leaving me only two months to collect experimental data.
I worked closely with Alix Merolle, who is in her first year of a PhD program, and we had weekly meetings with the Rubidium team to share our progress and address any issues we encountered. The experimental setup was mostly complete upon my arrival, so my role involved making a few upgrades and collecting and treating experimental data to assess the feasibility of Alix's planned experiment. We also spent considerable time discussing the future of the experiment, particularly in light of the upcoming move, as the setup will need to be reconstructed.
I greatly appreciated working with Quentin and Alix and sincerely thank them for their support and collaboration.

1 Introduction

During my internship at the LKB, I had the privilege of working with a team investigating the propagation of light in hot Rubidium (Rb) vapor cells. This research is exciting as it allows us to explore the physics of cold atoms indirectly. By using the Gross-Pitaevskii equation, traditionally applied to Bose-Einstein condensates (BECs), we draw an analogy between BEC dynamics and light propagation in Rb vapor. This remarkable correspondence opens up new avenues for studying nonlinear optical phenomena and quantum behaviors in a regime that has not been extensively explored.
At this early stage of our experiment, we are primarily focused on understanding the effects of the dispersive medium on light propagation. This foundational work is crucial for predicting and controlling the dynamics in future experiments. By investigating how light interacts with the hot rubidium vapor, we aim to accurately characterize our system. This understanding will set the stage for more complex studies involving the propagation of light pulses and broaden the range of phenomena we can explore.
The team has extensively explored the propagation of light in a plane under steady-state conditions (2D). Alix now aims to focus on the propagation of light in one dimension using pulses to observe dynamic behaviors. Instead of using a camera to image the plane, we use a photodiode to measure the intensity of the entire plane. This approach allows us to study the 1D dynamics of the system by capturing the overall intensity rather than detailed 2D images. This exploration of 1D dynamics is crucial for understanding quantum fluids, especially since superfluidity has never been observed in 1D physics.
In this report, I will detail the theoretical framework, experimental setup, methodologies, and preliminary findings of our investigation into 1D light pulse propagation in hot rubidium vapor cells. I will as well briefly talk about the long term objective of the experiment.

2 Theoretical background

The objective of our experiment is to study the propagation of light in a Rb vapor which is a dispersive medium. This kind of system can be easily described in a 3D space using Maxwell's equation in matter. Our specific case corresponds to a medium with no free charge and no free current and we hypothesise that there is no magnetization appearing. The system of equation characterizing our system is so [1]:

$$\nabla \times \mathbf{E} = -\frac{\partial \mathbf{B}}{\partial t} \qquad \nabla \cdot \mathbf{D} = 0 \tag{1}$$

$$\nabla \times \mathbf{H} = \frac{\partial \mathbf{D}}{\partial t} \qquad \nabla \cdot \mathbf{B} = 0 \tag{2}$$

$$\mathbf{D} = \varepsilon_0 \mathbf{E} + \mathbf{P} \qquad \mathbf{H} = \frac{1}{\mu_0}\mathbf{B}. \tag{3}$$

By applying a rotational on the first equation and using the following vector calculus identity, we can derive the so called Helmholtz equation [2]:

$$\nabla \times (\nabla \times \mathbf{A}) \;=\; \nabla(\nabla \cdot \mathbf{A}) \;-\; \nabla^2 \mathbf{A} \tag{4}$$

$$\nabla^2 \mathbf{E} - \frac{1}{c^2}\frac{\partial^2 \mathbf{E}}{\partial t^2} = \frac{1}{\varepsilon_0 c^2}\frac{\partial^2 \mathbf{P}}{\partial t^2}. \tag{5}$$

In this equation the dielectric polarization $\mathbf{P}$ appears. Dielectric polarization in an atomic gas occurs when the atoms' electron clouds shift slightly in response to an external electric field, creating induced dipoles. This means the positive and negative charges within each atom are displaced relative to each other. As a result, the gas acquires an overall dipole moment, which affects how it interacts with electric fields and electromagnetic waves, influencing properties like light propagation and absorption. In our case, the electric field will be the light wave and so its propagation will change with respect to our medium. Now let's consider an atomic vapor so an isotrope and centrosymetric medium, and a monochromatic polarized field:

$$\mathbf{P}(\mathbf{r}, \omega) = \epsilon_0[\chi^{(1)}(\mathbf{r}, \omega)\mathbf{E}(\mathbf{r}, \omega) + 3\chi^{(3)}(\mathbf{r}, \omega)|E(\mathbf{r}, \omega)|^2 \mathbf{E}(\mathbf{r}, \omega)] \tag{6}$$

$$\mathbf{E}(\mathbf{r}, t) = \frac{1}{2}(\mathcal{E}(\mathbf{x}, z)e^{i(k_0 z - \omega_0 t)} + c.c.)\mathbf{u_x} \text{ with } \mathbf{x} = (x, y). \tag{7}$$

The $\chi^{(3)}$ component represent the very known Kerr effect. Assuming the envelope does not vary in time (which is wrong but highly simplified the maths), and by combining equations 5,6 and 7, we can find:

$$\nabla^2 \mathcal{E}(\mathbf{r}, \omega_0) + k^2(\omega_0)\mathcal{E}(\mathbf{r}, \omega_0) + i\alpha k(\omega_0)\mathcal{E}(\mathbf{r}, \omega_0) = -\frac{3}{4}\frac{\omega_0^2}{c^2}\chi^{(3)}(\omega_0)|\mathcal{E}(\mathbf{r}, \omega_0)|^2 \mathcal{E}(\mathbf{r}, \omega_0). \tag{8}$$

In this equation we define the wavenumber $k(\omega) = k_0 n'(\omega))$ and the linear absorption coefficient $\alpha = 2k_0 n''(\omega)$ with $n(\omega) = \sqrt{1 + \chi^{(1)}(\omega)} = n'(\omega) + in''(\omega)$ being the linear

medium index. As $\alpha \ll k$ in the regime we are interested in, we can approximate $1 + \chi^{(1)}(\omega) \simeq k^2(\omega) + i\alpha(\omega)k(\omega)$. Then, using the slowly varying envelope approximation and the paraxial approximation ($\nabla^2\mathcal{E} \simeq 2ik\frac{\partial\mathcal{E}}{\partial z} + \nabla_\perp^2\mathcal{E}$), we can find:

$$i\frac{\partial\mathcal{E}}{\partial z} = -\frac{1}{2k(\omega)}\nabla_\perp^2\mathcal{E} - i\frac{\alpha}{2}\mathcal{E} + g(\mathbf{r},t)|\mathcal{E}|^2\mathcal{E}. \tag{9}$$

In this equation we introduce the non-linear interaction term $g(\mathbf{r},t) = -\frac{3k_0\chi^{(3)}(\omega_0)}{8n(\omega_0)}$. In all this discussion, I considered a time-independent envelope and monochromatic light for simplicity in calculations. However, it is important to remember that we are ultimately interested in the propagation of pulses in a 1D dispersive medium. Strictly monochromatic light does not exist, and pulses introduce additional spectral components. To accurately account for these effects, we need to include spectral dispersion in the derivation of the equation. This work has been addressed in the article [3]. With these time-dependent extra terms, the 3D NLSE propagation equation becomes:

$$i\frac{\partial\mathcal{E}}{\partial z} = -\frac{1}{2k(\omega)}\nabla_\perp^2\mathcal{E} + \frac{D_0}{2}\frac{\partial^2\mathcal{E}}{\partial t^2} - \frac{i}{v_g}\frac{\partial\mathcal{E}}{\partial t} - i\frac{\alpha}{2}\mathcal{E} + g(\mathbf{r},t)|\mathcal{E}|^2\mathcal{E}. \tag{10}$$

Let's now analyze the new terms involved in this equation. The group velocity, v_g, is defined as $v_g = \left(\frac{\partial k}{\partial\omega}\right)^{-1}(\omega)$ and represents the speed at which a pulse with a pulsation ω travels through the medium. Another important term is the group velocity dispersion (GVD), denoted as D_0. It is defined as $D_0 = \frac{\partial^2 k}{\partial\omega^2}$ and describes how the pulse centered on ω spreads during its propagation.
Now that we have the 3D propagation equation, let's simplify it by considering only two dimensions: the z-axis and time. Within the adiabatic approximation (where the transverse evolution is much smaller than the longitudinal one [4]) and following derivation in [5], we define the function Ψ to represent the longitudinal motion.

$$\mathcal{E}(\mathbf{x},z,t) = \Psi(z,t)\Phi(\mathbf{x};|\Psi(z,t)|^2). \tag{11}$$

If we now look at the dynamics of Ψ instead of $\mathcal{E}$, we get the propagation equation:

$$i\frac{\partial\Psi}{\partial z} = \frac{D_0}{2}\frac{\partial^2\Psi}{\partial t^2} - \frac{i}{v_g}\frac{\partial\Psi}{\partial t} + g_{1D}|\Psi|^2\Psi + \kappa_0\Psi. \tag{12}$$

One can remark that in this equation I removed the absorption of the field by the atoms. In fact as we only look at the two dimensions z and t, we can get rid of absorption with a renormalization processs of the field as it does not change the dynamics of the propagation. In this equation new terms appear: κ_0 plays the role of the fundamental transverse mode energy and g_{1D} is the non-linear interaction term reduced to one dimension.
In order to get even closer to the famous Gross-Pitaevskii equation, we can define the effective time τ, the effective comoving length ζ and the effective mass m as:

$$\tau = \frac{z}{v_g} \qquad \zeta = v_g t - z \qquad m = -\frac{\hbar}{v_g^3 D_0}. \tag{13}$$

Thus the equation become:

$$i\hbar\frac{\partial\Psi}{\partial\tau} = -\frac{\hbar^2}{2m}\frac{\partial^2\Psi}{\partial\zeta^2} + g_{1D}|\Psi|^2\Psi + E_0\Psi. \tag{14}$$

This equation is exactly the time-dependant Gross-Pitaevskii equation. To have a clear understanding of this analogy between light propagation in the medium and Bose-Enstein condensate (BEC) dynamics, analysing each term of the Gross-Pitaevskii equation and where they come from can be a great help.
In this equation, as the effective time τ is related to the z-axis, so it is crucial to understand that the dynamics could be observed in the different slices of the z-axis. However, as the cavity length cannot be changed and the imaging is set after the cavity We will be only able to observe the shape of the pulse after the cavity and not really the dynamics. The 2D team managed to find a trick to observe the dynamics of the fluid of light by playing on the intensity of light (and so the laser power). Details of this trick are in the section 1.2 of the thesis [2] for the interested reader. It would be interesting to discover if such a trick could be found in our case though.
Now let's talk about the wave function Ψ. In a BEC, this wave function is proportional to the root of the atomic density. In our case Ψ reveals the normalized amplitude of the total field on a slice z.
The mass in our fluid of light is determined by both the group velocity and the GVD. As equation 13 shows, a high GVD results in a low mass. But a low mass leads to strong dynamics since the system requires less energy to move. A high GVD is then very welcome in order to observe the dynamics.
The last important term is the interaction term $g_{1D}|\Psi|^2$, introduced by the Kerr effect in the nonlinear medium. By controlling this term through the power of our laser and the detuning from the Rb resonance, we can access a wide range of regimes in our system.

3 Experimental setup

The controllability of light is one of the fundamental strengths of our experimental approach. It is much easier to shape a pulse of light than creating matter wave moving along an axis for example. The ability to precisely emit and measure light makes it an ideal medium for probing the intricate dynamics of hot rubidium vapor cells. In our study, as said before, we focus on the propagation of a light pulse in a 1D configuration, so we do not have to shape a laser beam with a special light modulator, we should just focus on shaping a pulse. However, as we are at the very beginning of the experiment, we do not care in this report about the pulse shaping. We will emphasize the report on characterizing the medium. The following section will provide detailed descriptions of the experimental setup.
The light source is an external-cavity diode laser around 780 nm which allow a to tune the laser frequency down to tens of megahertz on large range (tens of GHz). This frequency tuning is done with a piezoelectric crystal changing the resonance cavity for the diode.
For the estimation of my laser frequency, I assume a linear relationship between the piezo

voltage and the laser frequency. While this approximation is not entirely accurate, it is straightforward to implement and provides a reasonable estimate for further calculations. The resulting error from this assumption is minimal, making it a useful method for obtaining initial frequency estimates. Saturation absorption spectroscopy (SAS) is used to accurately estimate the laser frequency for a specific piezo voltage, aided by a well-fitted curve.
SAS is a technique used to precisely measure the absorption properties of atomic vapors. It involves using two laser beams: a strong "pump" beam and a weaker "probe" beam, both directed through the vapor cell in opposite directions. In our case, this is the same beam retro-reflected. The pump beam excites a specific velocity class of atoms, saturating them, which reduces their ability to absorb light from the probe beam. This reduction in absorption creates a narrow dip in the absorption spectrum at the exact resonance frequency of the atomic transition, allowing us to get rid of Doppler broadening due to the transverse velocity of atoms [6]. A schematic representing this effect is given in figure 1. Analyzing these dips provides precise absorption frequencies, essential for fine-tuning lasers in experiments.

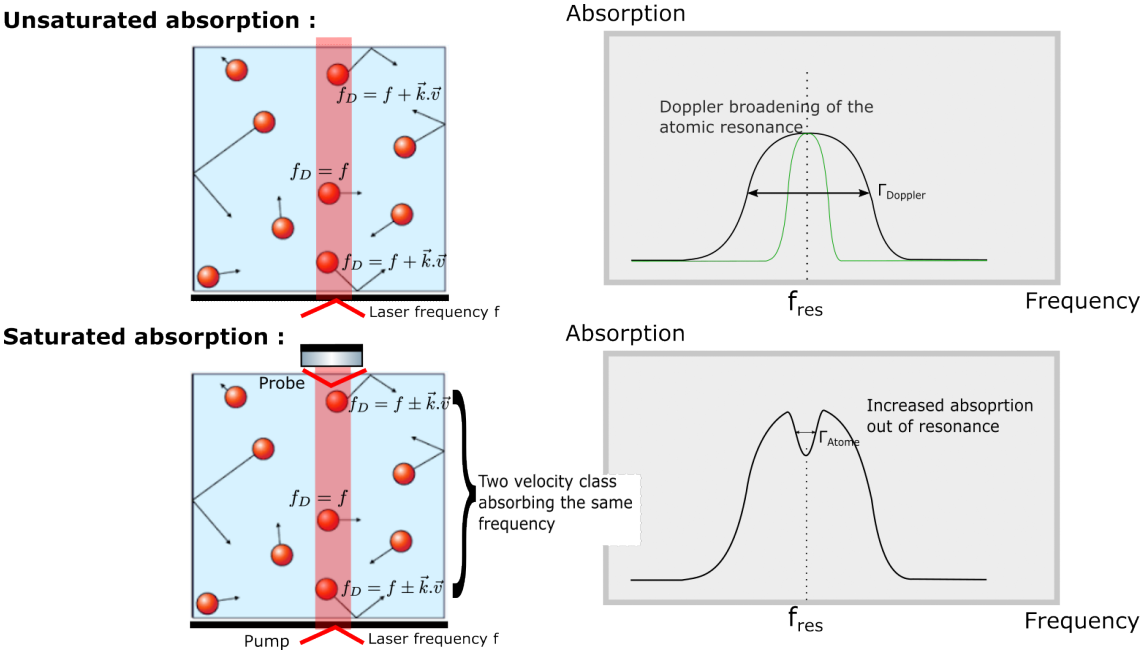

Figure 1: Schematic comparing SAS and a regular absorption spectroscopy.

The fit is then done using the known D2 lines of Rb for a natural Rb mixture [7]. More details about the atomic structure of Rb and its absorption spectrum is given in section 4. As the fit does not take into account a saturated absorption, we cannot see the dip of absorption that we have in the SAS experiment. A typical figure representing the result of this spectroscopy step is given in figure 2. Although this spectroscopy part will be probably improved after the moving the, the fit calculated is good enough to estimate

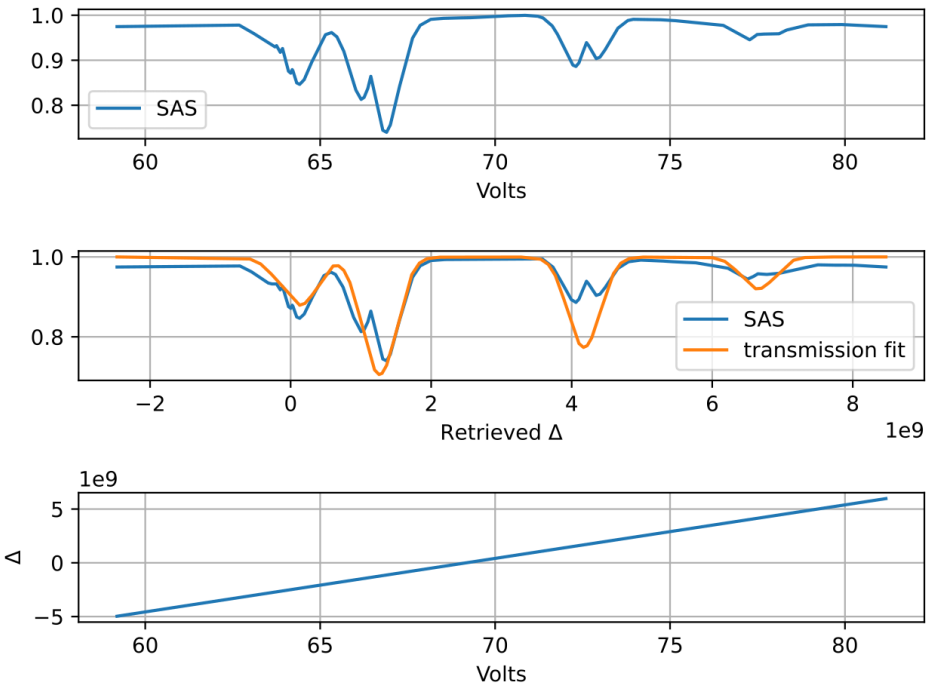

Figure 2: Typical SAS results : a) Fit of the SAS experiment with atomic absorption, b) Relationship found between light frequency and piezo voltage.

the relative frequency of our laser from resonance and have nice order of magnitude for the characterization of the atomic gas.
After this spectroscopy part, the light is sent to the optical table with an optical fiber. A Mach-Zehnder interferometer is then set with a Rb cell of 7.5 cm on one of the optical path. This setup is represented in figure 3. The cell is heated by two resistors controlled by a voltage power supply. Thanks to the interferometer we can measure the phase difference between the two optical path of the laser beam. Hence, we can estimate changes in the refraction index (see section 5). An improvement that I have made is the setup and the calibration of the two photodiodes before and after the cell. These photodiodes allow to measure the absorption of the atomic gas (see section 4).

4 Absorption

Absorption spectroscopy (or transmission spectroscopy) is particularly useful in atomic vapor cell experiments for precise temperature measurement of the vapor. Knowing the cell's temperature is crucial, as it affects the refractive index of the gas and consequently the effective mass of the system. By analyzing the absorption spectra, we can determine the Doppler broadening of the absorption lines, which is directly related to the temperature of the atomic vapor. This method provides an accurate and non-invasive way to monitor

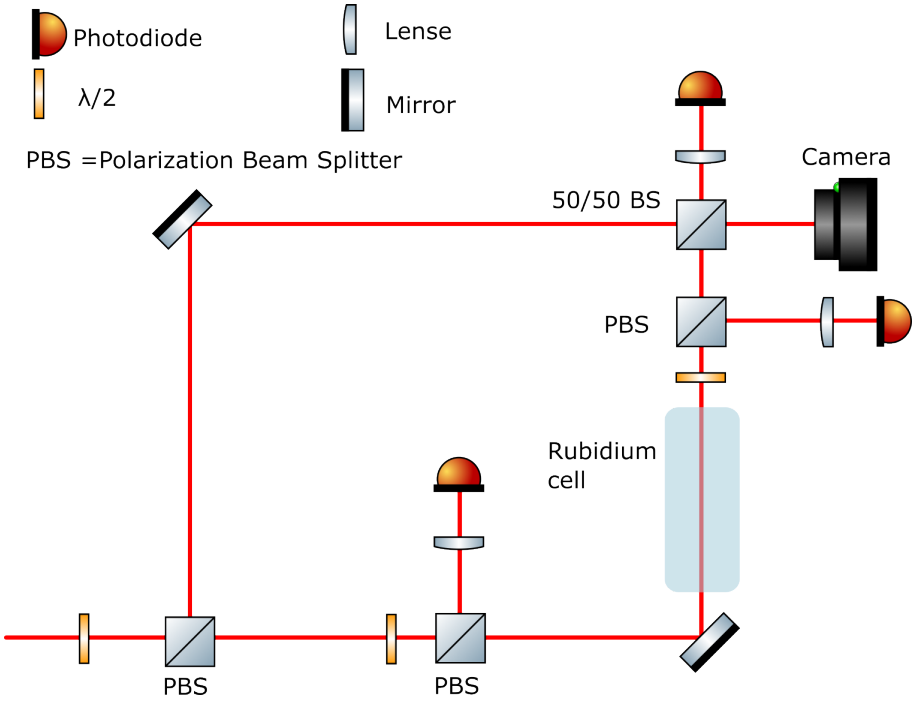

Figure 3: Experimental setup of the Mach-Zehnder interferometer.

and control the experimental conditions, ensuring reliable and reproducible results.
One of my tasks was to set up this absorption measurement system and implement the program to measure the temperature. In practice, I have set a transmission measurement but both are immediately related as $T = 1 - A$.

4.1 Rb spectrum

Rb is an atom with 37 protons and has two predominant natural isotopes. The most common isotope, ^{85}Rb, is stable and constitutes 72.17% of a natural mixture. The other predominant isotope, ^{87}Rb, is radioactive and makes up the remaining 27.83%. Other isotopes of rubidium are rare and will not be discussed in this report. Being an alkali metal, Rb has only one valence electron, giving it a simple atomic structure as shown in Figure 4.
In our experiment, we focus on the D2 line using a laser around 780 nm. With a natural mixture of rubidium, which is present in our cell, we observe four resonance peaks in the spectroscopy experiment of the D2 line. Each isotope has two hyperfine level resonances. A theoretical spectroscopy of the D2 line is shown in Figure 5. Each peak is labeled and can be correlated with the ground state levels depicted in Figure 4.

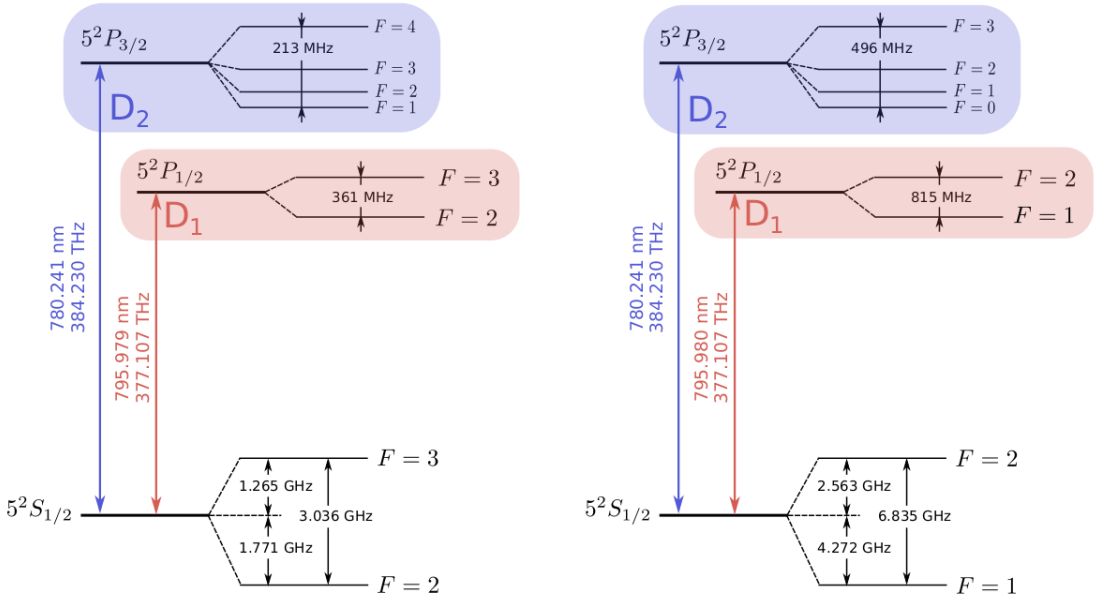

Figure 4: Rb hyperfine atomic structure for ^{85}Rb (on the left) and ^{87}Rb (on the right) and its D1 and D2 atomic transitions. Image from [8].

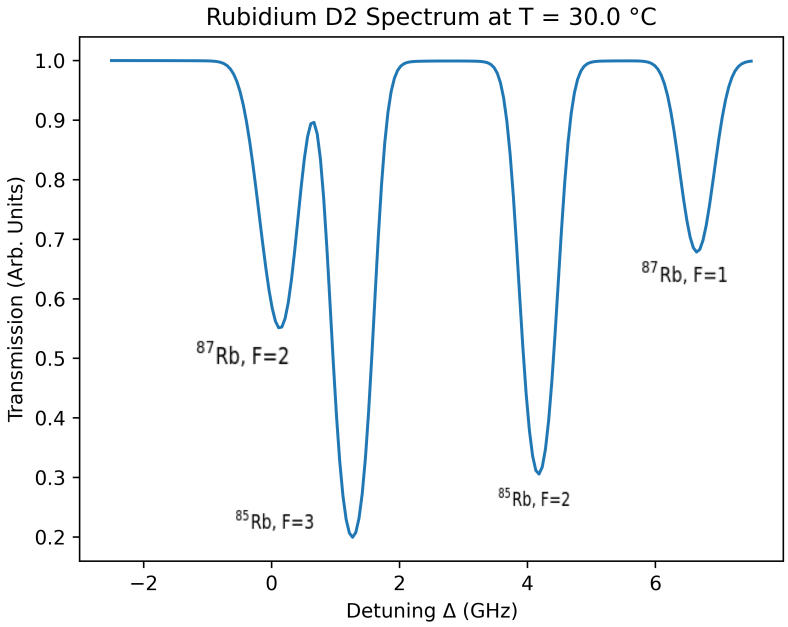

Figure 5: Theoretical spectroscopy of the D2 line of a natural Rb mixture at 30 °C based on the article [7].

4.2 Temperature measurement

Using a code based on the article [7], I can estimate the transmission of my cell based on the mixture and temperature set in the program (The figure 5 comes from this program). With photodiodes I have installed, I can then fit the measured transmission to the theoretical transmission and accurately estimate the temperature of the gas in the cell.
To accurately estimate the transmission of the cell, I first calibrated the two photodiodes around it. The input photodiode, located in the center of Figure **??**, was calibrated by measuring the output voltage for a set of light power levels at the entrance of the cell. A linear fit of this data allowed us to determine the input power based on the photodiode voltage. The same calibration process was performed on the second photodiode by measuring the power just after the cell. Once this calibration is made, transmission can be trivially obtained with : $T = \frac{I_{out}}{I_{in}}$.
Unfortunately, a with this calculation, it is impossible to observe a full transmission of the light even far from resonance. I believe this effect is due to reflections from the glass cell, which are likely not negligible. Additionally, I observed dips in the transmission when the cell was perfectly perpendicular to the laser beam. This dip, characteristic of saturated absorption, supports the hypothesis that glass reflections are indeed affecting the measurements to some extent. In order to avoid this saturated absorption effect, I tilted the Rb cell. A typical result of this transmission measurement is given in figure 6. We can indeed observe that the transmission is never reaching 1. Thus I artificially set the maximum of transmission to 1.

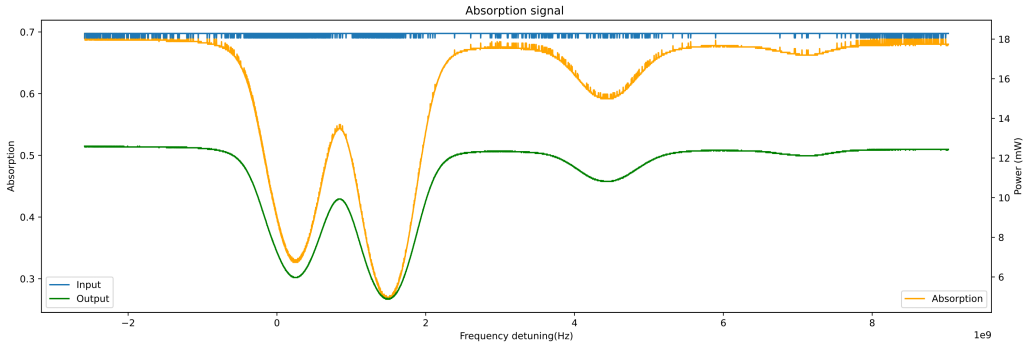

Figure 6: Typical results of a transmission measurement for the Rb cell at room temperature with 18 mW in input power.

We can also remark that in our measure the two dip at the right corresponding to ^{85}Rb, F=2 and ^{87}Rb, F=1 resonance are much less significant than in the theoretical model shown in figure 5. This effect is due to the atomic saturation. In fact, as the resonance strength factor for is higher for ^{87}Rb, F=2 than for F=1 and in a same way it is higher for ^{85}Rb, F=3 than for F=2 [7], the saturation does not allow to excites ^{87}Rb, F=1 properly (resp. ^{85}Rb, F=2). It is easy to get rid of this saturation effect, we just need to lower the power under the saturation intensity.

Once the transmission sprectum correspond to the atomic response, the fit is done using the program calculating the theoretical transmissions. In this temperature fit, there is three main steps. First, I do a temperature estimation by fitting the theory with the data. Then as the frequency fit process explained in the section 3 is not perfect, I do a new frequency fit of the transmission data on the theoretical transmission with the temperature estimation. Finally, I fit once again the theoretical model on the data with a new frequency axis in order to have a good temperature estimation. The figure 7 shows the final result of this fitting process for two different voltage of the resistor (and so two different temperatures of the cell).

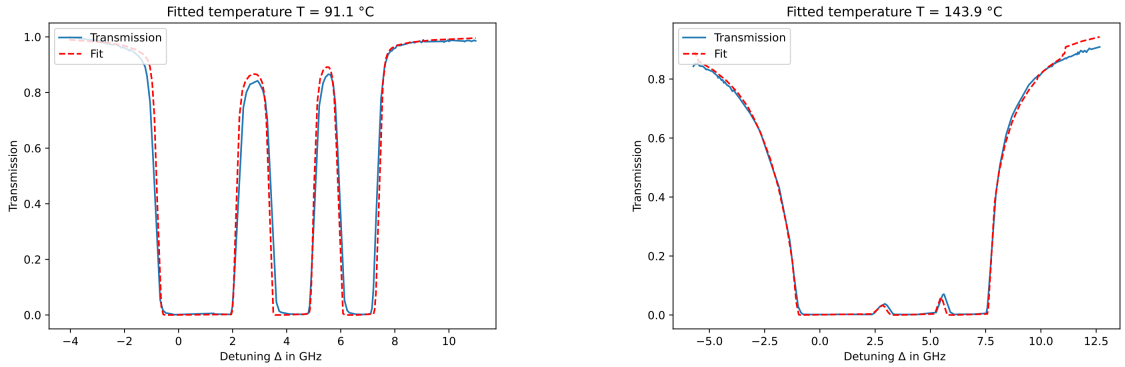

(a) Temperature fit at 10 V.

(b) Temperature fit at 15 V.

Figure 7: Fit of the experimental transmission data with the theoretical model. The fit is performed for two different resistor voltages: 10 V in Figure 7a and 15 V in Figure 7b. Note that the fit is less accurate in Figure 7b, as the detuning exceeds the range for which the code is designed.

In order to have an idea of the temperature response depending on the voltage set on the resistor, I measured by the way explained previously the temperature for a set of resistor voltage. This measures are represented in figure 8. We have to keep in mind that this trend represented is just an order of magnitude and as I did all the measures the same afternoon, I might have not waited long enough to be sure that the cell temperature is at steady state. This uncertainty on the fact that I reached the final temperature of the cell or not is the main reason I have high uncertainties on the cell temperature. This measures has been made just before the moving so I could not obtain a better dataset later. It is important to make this measurement again once the moving finished.

5 Group velocity dispersion (GVD)

As explained in section 2, GVD is directly related to the mass of our system. Hence, measuring GVD is crucial for accessing to the dynamics of our system. For instance, one of our objectives is to measure the Bogoliubov dispersion. For such a measurement a possibility if to perform a Bragg spectroscopy [9]. As said before the higher the GVD is,

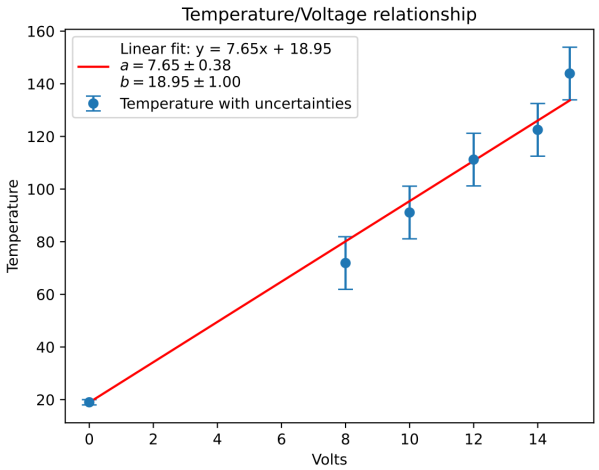

Figure 8: Temperature of the cell depending on the voltage applied on the resistor.

the stronger the dynamics is. Alix has been simulating this Bragg spectroscopy experiment considering the usage of an EOM around 100 MHz. We would like the GVD not to differ more than 5 % ovar these 100 MHz sidebands. Hence, we would like to have the highest GVD possible that does not change more than 5 % of its value over 100 MHz. While she worked on her simulations, I focused on measuring this critical GVD.
For the next part, a good understanding of what is GVD and how to calculate it is necessary. The GVD refers to the fact that different wavelength have different speed in a dispersive medium. Hence, the pulse will not only spread with propagation but a frequency chirp will appear as we can see on the sketch figure 9. We recall that GVD is defined by $D_0 = \frac{\partial^2 k}{\partial \omega^2}$. This expression is easy but unfortunately it is not really convenient to access to GVD by direct measurements. As the refractive index of the medium is accessible by measuring dephasing due to the cell, a more convenient formula for GVD using refractive index is :

$$D_0 = \frac{1}{c}\frac{dn_g}{d\omega} \qquad\qquad n_g = n + \omega\frac{dn}{d\omega} = \frac{c}{v_g}. \tag{15}$$

Here, we have defined the group refractive index,n_g , which basically reveals how fast is a pulse compared to light in vacuum. We can see that the observable we are interested in are easily accessible if we can measure properly the group refractive index n_g for a range of frequency.

5.1 Interferometry measurement

As shown in Figure 3, we measure the intensity of the light exiting the Mach-Zehnder setup using a couple of lenses and a photodiode. When the interferometer is properly aligned, with the two outgoing beams sharing the same optical axis, we should observe

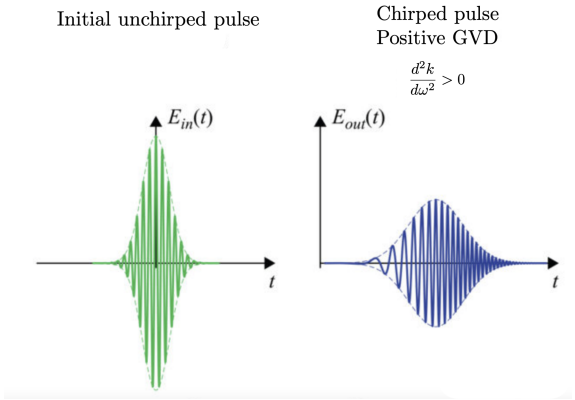

Figure 9: Sketch representing the evolution of a pulse in a dispersive medium.

large interference circles. The photodiode will then measure the light intensity of the zero-order interference. The intensity output of such an interferometer is given by:

$$I(\phi) = I_0 + I_1 + \sqrt{I_0 I_1}\cos(\Delta\phi) \tag{16}$$

where I_0 and I_1 are the intensities coming from the different path of the interferometer. The phase difference $\Delta\phi$ between the two optical path is determinded by :

$$\Delta\phi = L_{cell}(n-1)\frac{\omega}{c}. \tag{17}$$

With such an interferometer, two methods exist for measuring the group refractive index. One method involves measuring the phase and then determining n_g from n , while the other is called the zero-crossing method and concist on using maxima and minima of the inteference pattern. Both methods require measuring the phase difference from the interferometer. As determining GVD from n_g is not really a problem, the two following subsections will focus on obtaining n_g with the two different methods.
Before digging in how to obtain n_g, it is important to have an idea of what is the signal that we can observe after the interferometry measurement. Such a signal is shown in figure 10. Several observations can be made from this figure. Firstly, as we approach resonance, the impact of detuning on the interference pattern increases. This is because the refractive index rises, and thus its dependence on frequency becomes more significant, as shown in equation 17. Then we can see that, once again, the frequency estimation is not perfect as with no detuning we should not be able to observe any interference, the Rb cell should absorb all the light. After the moving it will be really necessary to improve detuning estimation.

5.1.1 Zero-crossing measurement

Zero-crossing method is the less obvious method in theory but the easiest to implement in this experiment. This method has been shown useful to measure the ground index in

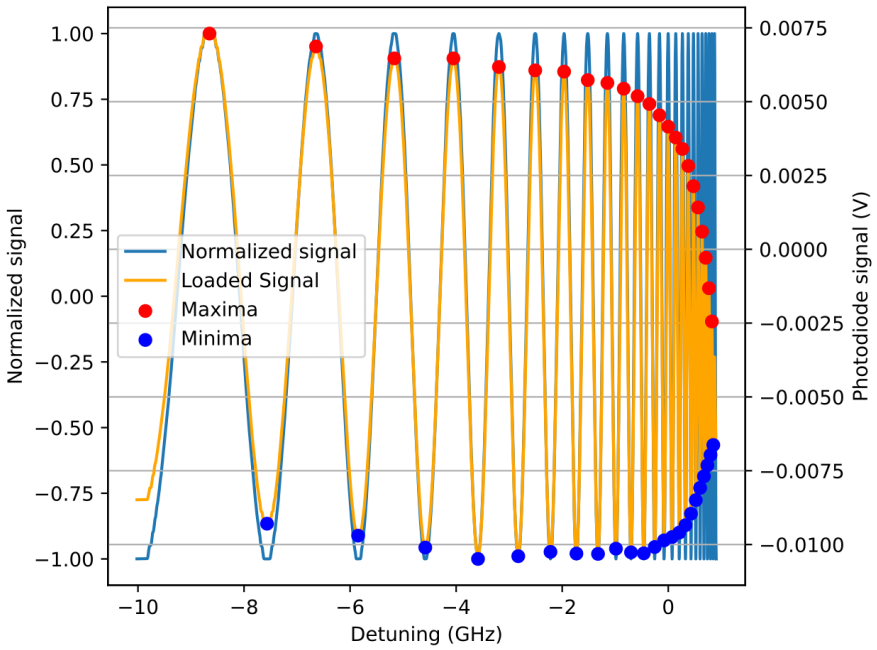

Figure 10: Interference pattern out of the photodiode (in orange) and its normalized version in blue. Maxima of the interference patter are represented on the signal. This data is taken with a power of 3 mW going through the cavity and a resistor voltage of 15 V (approximately 140 °C).

[10]. The idea is simple, once you have your interference signal you measure the maxima of the signal and from it, compute the group index using the Fabry-Perot formula :

$$n_g = \frac{c}{2L_{cell}\Delta\nu}. \tag{18}$$

We can remark that they used the Fabry-Perot formula where in our experiment we are using a cell and not a cavity. I verified that the formula should stay the same in our case and it works. This method is really straightforward to implement as finding the maxima and minima of a signal can be done easily if the signal is properly filtered. I used a gaussian filter in order to get rid of the photodiode noise on figure 10 and one can see that maxima determination correspond to what we can observe on the signal. The results for the group index found by this method are given by the red dots on figure 12. The problem with this method is that we do not obtain a continuous idea of the value of n_g, and so the estimation of the GVD is discrete too.

5.1.2 Phase unwrapping measurement

The other method in order to obtain a continous estimation of the GVD is to estimate the phase for the whole set of frequency in the data set and to "unwrap" it, that means

the phase is continusously increasing instead of staying between 0 and 2π.
This phase unwrapping has been a pain as I tried many different things and methods were highly depending of the initial data. Using Hilbert transform was promising on the beginning but I always had strong edge effects and then n_g was not perfectly representative of the atomic characteristic.
The most effective method involved normalizing the signal and then evaluating the phase of this normalized signal. This process requires several steps. Initially, I attempted to extract I_1 and I_0 to isolate the $\cos(\Delta\phi)$ term, but this approach did not work as expected for reasons I could not determine. The best results were obtained by normalizing the signal based on previously estimated maxima and minima, setting all maxima to 1 and all minima to -1.
The only problem with this method is that we have edge effects (but contained on the first and the last half period) and if the maxima and minima detection is not perfect, we have issues obtaining the phase estimation. It is the best solution I found for the normalization though. The signal obtained after this process is given in blue in figure 10.
The phase evolution can then be obtain using a simple arccos function. After this part we then have a signal oscillating between 0 and π. We then need to set a condition making this signal always increasing and changing the sign of the arccos output every half period. After this signal processing we can obtain the curve given in figure 11. The group index is then determined using :

$$\frac{d\phi}{d\omega} = L_{cell}\frac{n-1}{c} + L_{cell}\frac{dn}{d\omega}\frac{\omega}{c} = \frac{L_{cell}}{c}(n_g - 1). \tag{19}$$

One has to know that for the derivative of the phase, in order to get rid of the fluctuation of the phase around its trend, I used the function `UnivariateSpline(x,y,k,s)` from `scipy.interpolate` library. This interpolation function takes a set of data with x and y-values and interpolate using a Spline function [11]. Spline are a good way to extract a trend from data allowing in our case to select the polynomial degree of interpolation `k` and a smoothing factor `s`. The estimation of the group index is then represented in figure 12 in blue.

5.2 Results

Using the methods detailed in the previous subsections, we can estimate the group index n_g. These estimations is given in figure 12. Fortunately, we can observe that both methods give similar results ! GVD can be then easily calculated with the equation 15 for both zero-crossing and unwrapped phase method. A problem that we can have with the phase unwrapping method for GVD estimation is that the smoothing factor `s` needs to be very wisely chosen in order for the GVD estimation to follow properly the trend. A badly chosen smoothing factor can bring oscillations on the GVD estimation as in figure 14. But a nicely chosen `s` gives a nice estimation of the GVD at the end of all this data processing as figure 13 can witness. For all the resistor voltage that I tried, I managed to measure at most the order of 10^{-15} s^2/m. It is nice to compare this GVD with the standard GVD of an optical fire : 10^{-25} s^2/m Next step will be to know if it is enough to perform a Bragg spectroscopy.

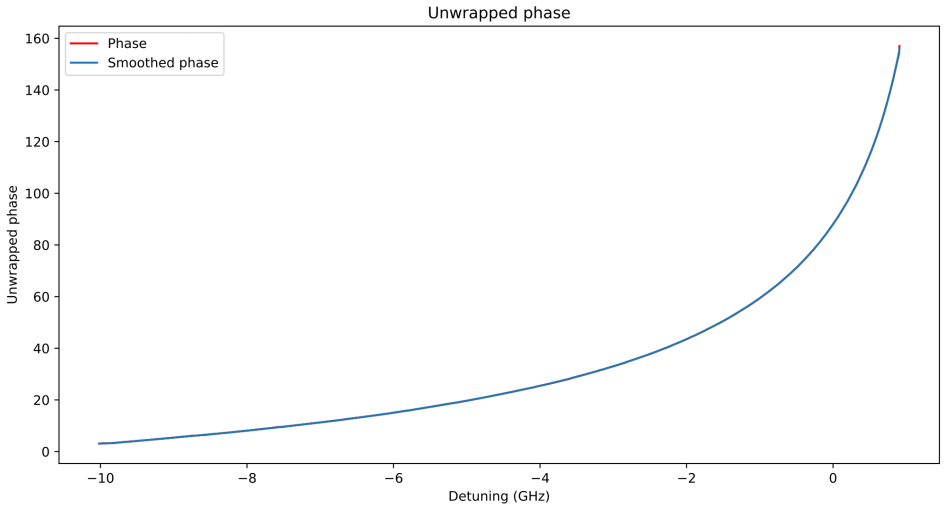

Figure 11: Estimation of the evolution of the phase difference of the data represented in figure 10.

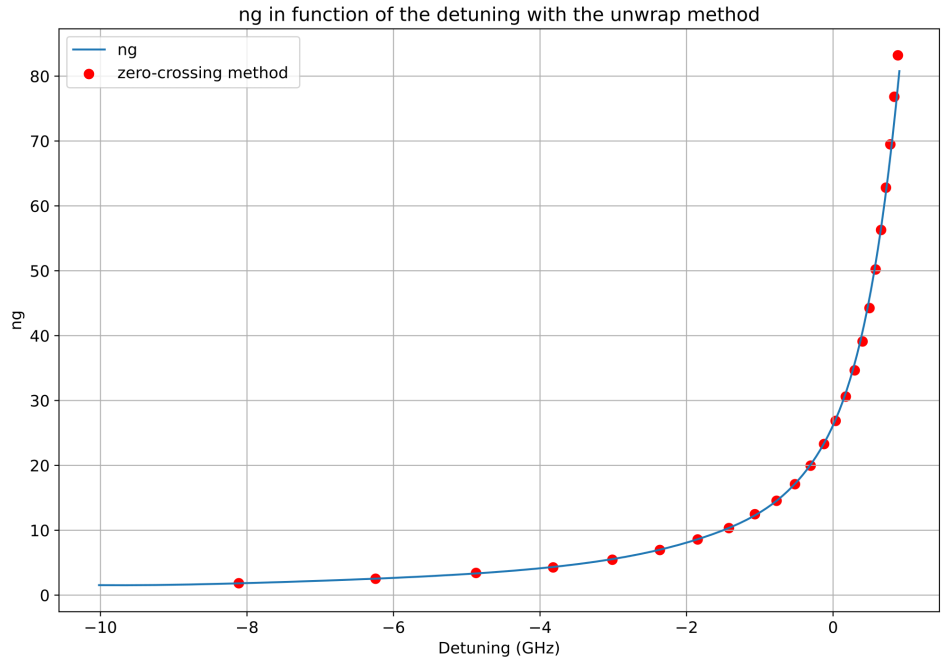

Figure 12: Results found for the group index n_g with the two different methods : Phase unwrapping (in blue) and zero-crossing (red dots). The data used to extract this group index is the data of figure 10.

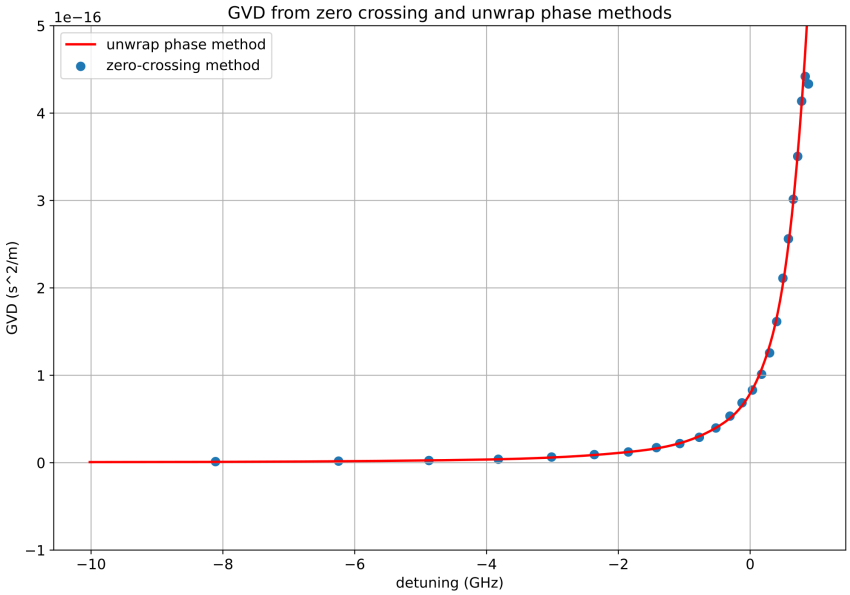

Figure 13: GVD extracted from the data represented in figure 10.

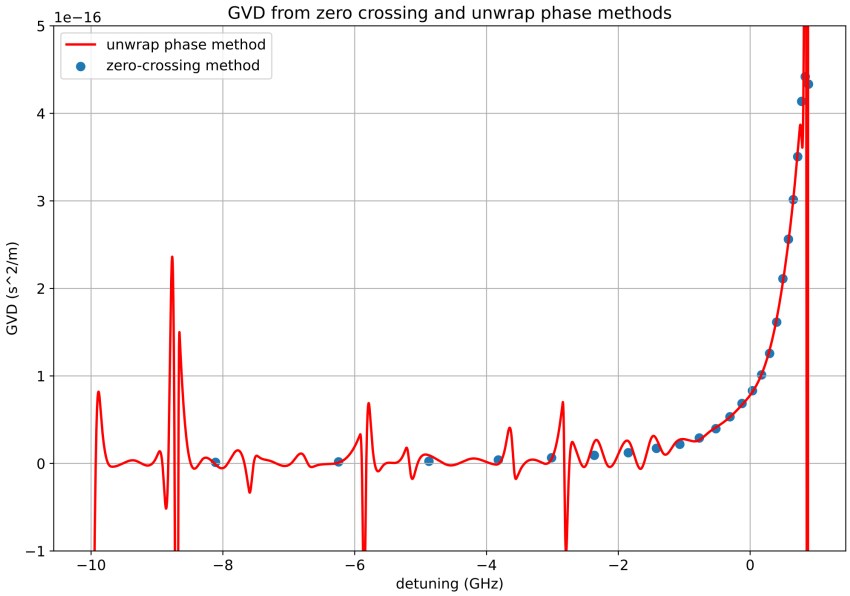

Figure 14: Example of an oscillating estimation of the GVD caused by a wrongly chosen smooting factor `s`. The data used is the same as in figure 13.

6 Conclusion

To conclude, in this report we explored effective methods for characterizing a dispersive medium. We demonstrated how to accurately estimate the temperature of the gas using a theoretical absorption model. Additionally, we reviewed two different methods for estimating the refractive group index and the GVD of the medium, obtaining coherent and reliable results. By accurately estimating the GVD, we gained insights into the dynamics of our system through simulations. This characterization was essential before beginning pulse propagation experiments, as it helped us determine the optimal regime for future experiments, including the appropriate laser frequency and temperature. Moreover, the versatility and reliability of our characterization techniques will be valuable for future experiments. Knowing the precise characteristics of the medium will enable the repeatability of future experiments, which is a key aspect of research.

During this internship, I gained substantial experience in data analysis and improved my programming skills. I also discovered the field of quantum fluids in hot cells. I particularly appreciated the shift from working with cold atoms, which require massive experimental setups, to this field, which involves simpler setups while still introducing a wealth of intriguing physics.

Thanks to this work, Alix will be able to explore 1D quantum fluids, a research field that requires further insight. For instance, superfluidity in a 1D quantum fluid has yet to be observed.

The next steps for the experiment include upgrading to a more powerful laser to introduce strong non-linearity, improving the frequency measurement of the laser by making it interfere with another stabilized laser, and finally doing a Bragg spectroscopy of this 1D fluid of light.

I greatly appreciated working with this team. I learned a lot of new physics and met very friendly people. The team was incredibly welcoming. Although I will be transitioning to environmental sciences next year, this experience has given me good memories of research in physics.

References

[1] D. J. Griffiths, "Introduction to electrodynamics." Cambridge University Press, 2023, ch. 7.3.5.

[2] T. Aladjidi, "Full optical control of quantum fluids of light in hot atomic vapors," Theses, Sorbonne Université, Oct. 2023. [Online]. Available: https://theses.hal.science/tel-04391272

[3] Y. Kodama and A. Hasegawa, "Nonlinear pulse propagation in a monomode dielectric guide," *IEEE journal of quantum electronics*, vol. 23, no. 5, pp. 510–524, 1987.

[4] P. Leboeuf and N. Pavloff, "Bose-einstein beams: Coherent propagation through a guide," *Physical Review A*, vol. 64, no. 3, Aug. 2001. [Online]. Available: http://dx.doi.org/10.1103/PhysRevA.64.033602

[5] P.-É. Larré and I. Carusotto, "Prethermalization in a quenched one-dimensional quantum fluid of light: Intrinsic limits to the coherent propagation of a light beam in a nonlinear optical fiber," *The European Physical Journal D*, vol. 70, pp. 1–19, 2016.

[6] D. W. Preston, "Doppler-free saturated absorption: Laser spectroscopy," *American Journal of Physics*, vol. 64, no. 11, pp. 1432–1436, 11 1996. [Online]. Available: https://doi.org/10.1119/1.18457

[7] P. Siddons, C. S. Adams, C. Ge, and I. G. Hughes, "Absolute absorption on rubidium d lines: comparison between theory and experiment," *Journal of Physics B: Atomic, Molecular and Optical Physics*, vol. 41, no. 15, p. 155004, Jul. 2008. [Online]. Available: http://dx.doi.org/10.1088/0953-4075/41/15/155004

[8] Q. Fontaine, "Paraxial fluid of light in hot atomic vapors."

[9] J. Stenger, S. Inouye, A. P. Chikkatur, D. M. Stamper-Kurn, D. E. Pritchard, and W. Ketterle, "Bragg spectroscopy of a bose-einstein condensate," *Physical Review Letters*, vol. 82, no. 23, p. 4569–4573, Jun. 1999. [Online]. Available: http://dx.doi.org/10.1103/PhysRevLett.82.4569

[10] A. Papoyan, S. Shmavonyan, D. Khachatryan, and G. Grigoryan, "Straightforward retrieval of dispersion in a dense atomic vapor helped by buffer gas-assisted radiation channeling," *J. Opt. Soc. Am. B*, vol. 34, no. 4, pp. 877–883, Apr 2017. [Online]. Available: https://opg.optica.org/josab/abstract.cfm?URI=josab-34-4-877

[11] S. McKinley and M. Levine, "Cubic spline interpolation," *College of the Redwoods*, vol. 45, no. 1, pp. 1049–1060, 1998.